Apoptotic Gene Expression of the AP-1 Transcription Factor in IRBP $^{-/-}$ Mice

By
Paul Chung
April, 2018



Allegheny College
Department of Biology

Apoptotic Gene Expression of the AP-1 Transcription Factor in IRBP $^{-/-}$ Mice

By
Paul Chung
April, 2016

A Senior Comprehensive Project in Partial Fulfillment of the Requirements
for a Bachelor of Science Degree from Allegheny College

I hereby recognize and pledge to fulfill my responsibilities as defined in the Honor Code
and to maintain the integrity of both myself and the College community as a whole.

_____
Pledge

Approval by the Senior Thesis Committee:

_____
Dr. Donmoyer

_____
Dr. Nelson

Table of Content

Acknowledgement..……..……...1

Abstract……...……..…..2

Introduction……...…….……3

Methods……...……..……...…9

Results……..……...…..14

Discussion……..……...20

Literature Cited……..…….....…23

Appendices……...…….……...….26

Aknowledgement

I would like to thank the following people for giving me support and care in completion of this project.

Dr. Donmoyer: I would like to thank Dr. Donmoyer for having me in her comp group. She has given me the best advice I needed and emotional support and encouragement. Thank you for always answering my last minute questions. I will be grateful for the experiences I have had in your lab from junior seminar to my senior comp. I will continually use the skills and advices that you have taught me in all my life. With your teachings, I feel more ready to have a career in medicine and face further challenges in my life.

Dr. Nelson: Thank you for having me in your lab ever since my first year in Allegheny College. It was unfortunate that I never was in any of your classes. However, you are one of the most influential people in my life. I feel that I have built a strong foundation of skills required for laboratory work thanks to your teaching and utilized them in all of my other classes. Thank you for all the support you have given me.

Professor Lundberg: I am very grateful for the help and advice when I was unsure about my statistical analysis.

Elizabeth Caskey: Thank you so much for breeding and taking care of my mice. I wouldn't have been able to do my senior project without your care and support. Thank you for your constant communication to let us know whenever new litters were born.

Classmates: Sam Thomas and Karla Atcheson, I would like to thank you guys for always giving me support and encouragements. During weekly comp meetings, you guys gave me feedback that would help me to clear up my thoughts. Thank you for all your support through out past four years.

Maggie Donaldson, thank you for your support in showing me how to set up a qPCR run. I am very grateful that you took your time off from doing your own project to help me out with mine.

Chioma Alaka, thank you for your huge support in teaching me how to do retinal dissection and RNA isolation techniques. I wouldn't have been able to do my comp without your lessons. I wish you the best of luck for your future comp.

Anna Meyer, thank you for being a supportive lab assistant. Thank you for your help in the dissection process.

Abstract

Activator Protein 1 (AP-1) is a dimeric transcription factor whose transcription rate is controlled by the Fos and Jun families. Fos and Jun families regulate structure and play a role in oncogenic transformation. In the retina, AP-1 transcription factor is stimulated by high intensity light, which induces photoreceptor apoptosis. A different mouse model, interphotoreceptor retinoid-binding protein-deficient ($IRBP^{-/-}$) mice were chosen due to its early photoreceptor degeneration. This research investigated if there are comparable proteins involved in apoptosis in $IRBP^{-/-}$ mice as observed in the light-induced model. Expression of c-Fos, pro-apoptosis gene bax, and anti-apoptotic gene Bcl-x_L were tested in $IRBP^{-/-}$ (n=3) and wild type (n=3) (WT) groups via quantitative polymerase chain reaction. Their retinal tissues were collected at postnatal day 25, which is near the peak of apoptosis. Tissues were homogenized and total RNA was isolated. Cycle threshold (C_t) was measured. ΔC_t was calculated for each gene by subtracting the average C_t of reference gene (18S ribosomal RNA) from the average C_t of the target gene. Multivariate analysis of variance (MANOVA) was used to analyze the data. P-value was 0.096 for all genes, which indicates that there is no significant difference between $IRBP^{-/-}$ and WT groups. A trend was observed where *c-Fos* was more expressed in the $IRBP^{-/-}$ group than the WT group. Since p-value is >0.05, there was no difference between genes *c-Fos, bax,* and Bcl-x_L, which suggests that apoptosis in 25-day-old $IRBP^{-/-}$ mice is not mediated by these genes.

Introduction

Inherited retinal degenerations cause loss of vision due to abnormalities in the retina. One form of retinal degenerative disease is retinitis pigmentosa (RP), a genetic disorder caused by loss of photoreceptor cells in the retina. Mutations in multiple genes that encode retinal proteins result in photoreceptor dysfunction. There are approximately 100,000 people affected by RP in the United States (National Eye Institute, 2014). RP symptoms such as blurred vision and tunnel vision (peripheral vision loss) usually begin in childhood or early adulthood. One of the causes for RP is a mutation in interphotoreceptor retinoid-binding protein (IRBP), which will be discussed later.

The retina is the innermost layer of the eye and contains two types of photoreceptors: rods, which detect dim light, and cones, which detect color in bright light. Both types of photoreceptors generate electrical signals via phototransduction by which visual signals are transduced. A derivative of vitamin A, 11-*cis* retinal, is needed for photoreceptors to detect light. When a photon of light is absorbed by 11-*cis* retinal, the molecule is photoisomerized to all-*trans* retinal. Then this molecular change is converted into an electrical signal.

Apoptosis

Apoptosis or programmed cell death can occur in response to stimuli, while necrosis is a form of cell death that is triggered by events such as trauma or infection. Unlike necrosis, apoptosis can induce cell death without such harmful triggers. Apoptosis is imperative for cell turnover, proper embryonic development, and proper functioning of the immune system (Elmore, 2007). It normally occurs to maintain cell populations in tissues by eliminating unwanted cells. For example, during embryogenesis, cells undergo apoptosis as a way to shape the normal adult form and suppress the formation of abnormalities such as having extra limbs or fingers

(Gavrilescu & Denkers, 2003). However, harmful cases of apoptosis can cause cancer, neurodegenerative diseases, and autoimmune diseases (Elmore, 2007). With regard to vision, loss of photoreceptors can be caused by the activation of genes that induce apoptosis (Grimm et al., 2000).

Cell death can be classified by different morphologies and biochemical mechanisms, which are described by the Nomenclature Committee on Cell Death. These include enzymological criteria, functional aspects, and immunological characteristics (Livingston, 1997; Kroemer et al., 2009). An example of enzymological cell death is when apoptosis is induced via activation of cysteine proteases or caspases. This activation can lead to cascades of events that produce signals to destroy the cell (Livingston, 1997). The cysteine protease gene family is known for executing apoptosis via breaking peptide bonds between cysteine and aspartic acid. A series of caspases such as caspase-3 and caspase-9 is involved in apoptotic pathways (Zhivotosky, 2003).

Caspases in the Retina

As mentioned above, programmed cell death often relies on activation of caspases. Caspases activation is observed in death of photoreceptors in retina, suggesting that retinal degeneration may be dependent on activation of caspases (Grimm et al. 2000). However, in the presence of caspase activity inhibitors, apoptosis was observed in retina. This result indicates that caspase-independent apoptosis can also occur in the retina (Doonan et al., 2003). After treating mice with a high intensity of light, there was an increase in caspase-1 activity (Perche et al., 2007). A significant increase in caspase-1 activity suggests that it might be involved in coordinating apoptotic cell death of photoreceptors after exposure to light.

Light-Induced Apoptosis

Apoptosis involving caspases is observed in retinas when photoreceptors are struck by high intensity visible light. The longer the duration of exposure and the higher the intensity of light, the more damage the photoreceptors will incur (Grimm et al., 2000). Photoreceptor degeneration is caused by Activating Protein-1 (AP-1) transcription factor, which regulates gene expression in response to high light intensity, is activated to promote photoreceptor apoptosis (Grimm et al., 2000).

AP-1 is a dimeric transcription factor that is controlled by proteins from the Fos and Jun families. Examples of Fos family members include c-Fos, FosB, Fra-1, and Fra-2, and examples of Jun family members include c-Jun, JunB, and JunD (Hafezi et al., 1999). Expression of Fos and Jun proteins is increased when stimulated by stressors such as UV light, cell proliferation, and apoptosis. Hafezi et al. analyzed AP-1 DNA binding activity and its complex composition in mouse retina during light-induced photoreceptor apoptosis (1999). After 6 hours of light treatment, antibody interference analysis revealed that the major composition of AP-1 were c-Fos and JunD heterodimers. They concluded that induction of AP-1 via light exposure may depend on a quantitative increase of c-Fos and JunD more than other members of Fos and Jun families.

Similarly, Grimm et al. used light treatment to study light-induced apoptosis in mouse retinas (2000). They exposed c-fos knockout (c-fos$^{-/-}$) and wild type (WT) mice with either 60 or 13,000 lux and measured the expression of *c-fos*, *c-jun*, *caspase-1*, and other pro- and anti-apoptotic genes. Results showed that c-fos, c-jun, and caspase-1 play significant roles in activating AP-1, causing photoreceptor cell death after light exposure. However, the other apoptotic genes had little to no change no change in gene expression such as *Bcl-2, Bcl-*x_L*, bax,*

and *bad*. A significant increase in caspase-1 mRNA level post light exposure may suggest that caspase-1 play significant roles in light-induced apoptosis. However, its relationship to the AP-1 pathway in retina is not well understood (Grimm et al., 2000). This treatment method is not practical because 13,000 lux is 65 times greater than the average room intensity (200 lux). Therefore, a different study model, using $IRBP^{-/-}$ mice, which are a model of early photoreceptor degeneration, was selected for this research. It is not known which apoptotic pathway $IRBP^{-/-}$ mice undergo. Perhaps they utilize the same apoptosis pathway as found in light-induced apoptosis. Therefore this research focuses on investigating whether $IRBP^{-/-}$ mice utilize the AP-1 pathway by testing for the same genes *c-Fos, caspase-1, Bcl-*x_L, and *bax.*

Role of IRBP

$IRBP^{-/-}$ mice have been previously used to study apoptosis of photoreceptors (Wisard et al., 2011; Homa, 2013; Turner, 2016). IRBP is a large glycoprotein secreted by photoreceptors into the interphotoreceptor matrix (IPM), which separates the retinal pigment epithelium (RPE) and photoreceptors (Keating et al., 2008). Part of the visual cycle, shown in Figure 1**,** IRBP mainly binds to 11-*cis* retinal in the dark and all-*trans* retinol in light-adapted eyes. This binding activity is important to carry these molecules across the interphotoreceptor space. After IRBP carries 11-*cis* retinal from RPE cells to rod outer segments, the aldehyde is bound to opsin to generate rhodopsin. Then in the presence of light, 11-*cis* retinal is photoisomerized to all-*trans* retinal, causing dissociation from the opsin. Next, a retinol dehydrogenase converts all-*trans* retinal to all-*trans* retinol (Pepperberg et al., 1993). IRBP carries all-*trans* retinol from rod outer segments through the IPM to the RPE. All-*trans* retinol is esterified, isomerized and oxidized back to 11-*cis* retinal to complete the visual cycle. The molecule gets transported across the IPM into rod outer segments again, where it binds to opsin and restores the content of the first reactant

in the visual cycle (Pepperberg et al., 1993). Therefore, IRBP plays a significant role in transporting key molecules leading to the restoration of rhodopsin.

Figure 1: Steps of the Visual Cycle

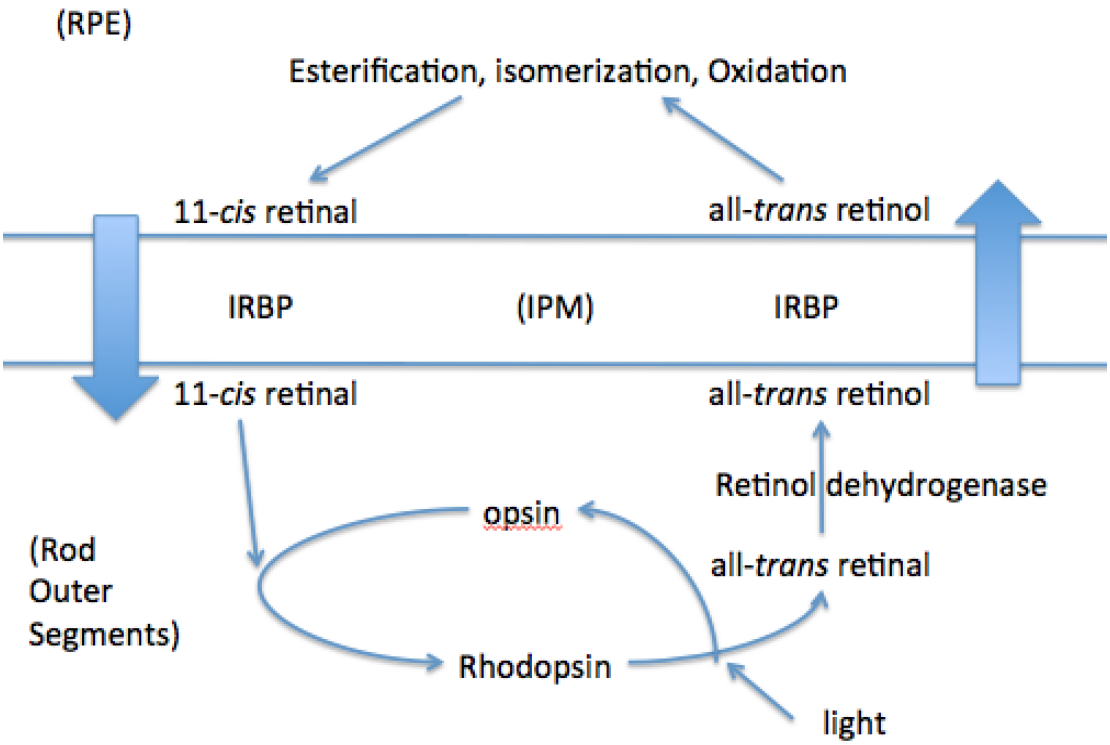

Studies with IRBP$^{-/-}$ mice reveal that IRBP plays a role in cone pigment regeneration (Parker et al., 2009). It is also possible that IRBP plays a role in early eye development as its mRNA is expressed at embryonic day 13 (Liou et al., 1994). If IRBP is involved in early eye development, then IRBP$^{-/-}$ mice should show abnormalities in eye development. Using IRBP$^{-/-}$ and C57BL/6J WT mice of varying ages, Wisard et al. showed that IRBP$^{-/-}$ mice experienced retinal degeneration from apoptosis at ~25 days of age (2011). They counted the number of retinal cells via bromodeoxyuridine (BrdU) labeling and measured the thickness of retinal cell layers from early stage (postnatal day p2) to adulthood (p440). They discovered that the retinas in IRBP$^{-/-}$ were 20% thinner, and at p30, there were 30% fewer cones than in age-matched WT

mice (Wisard et al., 2011). These findings showed that IRBP$^{-/-}$ mice aged between P23 and P30 had excessive retinal apoptosis, determined by terminal deoxynucleotidyl transferase (TdT) dUTP nick-end labeling (TUNEL) staining, compared to age-matched WT mice. Wisard et al. suggest that apoptosis plays a key role in the death of photoreceptors. Therefore, it is imperative to determine which pro-apoptotic and anti-apoptotic genes are involved in photoreceptor apoptosis induced by lack of *Irbp.* Having more understanding about photoreceptor apoptosis would provide knowledge to finding treatments to correct and prevent the degeneration.

This research predicted that activation of AP-1 transcription factor would be observed in IRBP$^{-/-}$ mice at P25 without light treatment. Therefore, there will be higher expression of caspase-1 and c-fos genes in IRBP$^{-/-}$ compared to WT mice. This research also tested pro- and anti-apoptotic genes that are involved in AP-1 transcription. The apoptosis agonist (favoring cell death) *bax* and antagonist (hindering cell death) *Bcl-x_L* were the two genes of interest in this study. *Bax* is a prop-apoptotic gene that induces cell death and is found in AP-1 apoptotic pathway (Ameyar et al., 2003). However, anti-apoptotic genes such as *Bcl-x_L* prevent apoptosis by interfering with steps that lead to activating caspases (Tsujimoto, 1998). Apoptosis antagonists also prevent the release of apoptosis-inducing factors (Liu et al., 1996). Hypothesizing that AP-1 apoptotic pathway occurs in IRBP$^{-/-}$ mice, this research also predicted that there would be higher expression of *bax* and lower expression of *Bcl-x_L* in IRBP$^{-/-}$ mice compared to age-matched WT mice.

Methods

Animals

The IRBP$^{-/-}$ strain was obtained from John Nickerson at Emory Eye Center, Atlanta, GA in 2010, and C57BL/6J mice came from the Allegheny College colony. Mice were fed Lab Diet 5P00 Prolab RMH 3000 (St. Louis, MO). They had free access to water and were exposed to 12:12 hours of light: dark environment.

Seven litters of 25 days old IRBP$^{-/-}$ mice and five litters of C57BL/6J wild type (WT) mice were collected. Five additional samples of practice tissue at various age and strain were collected. Therefore, a total of 17 litters were collected. Four of the five practice samples were used to improve dissection and RNA isolation techniques. Others were used to test primers. Some litters were pooled together to yield larger sample size because of lack of mice born in a litter. Three samples of IRBP$^{-/-}$ mice and three samples of WT mice were used for data collection.

Retinal Dissections

When mice reached postnatal day 25 (P25), they were sacrificed individually via 3 minutes of CO_2 inhalation in a chamber. After sacrifice, enucleation was done to obtain the eye. The eye was placed on a slide for dissection. Then microdissection was performed to collect retinas with a Lecia M80 microscope. A small incision was made on the anterior part of the eye with microdissection scissors. Then retinas were extracted from both eyes. Retinas from multiple mice were pooled into a 2mL centrifuge tube and placed on dry ice. After dissections were completed, the tube was stored in a -70°C freezer until RNA isolation was performed.

Homogenization

Trizol (500 µL; nvitrogen, Carlsbad, CA) was added to retinal tissue to enhance RNA stability. A Kontes pellet pestle motor and sterile disposable tip was used to homogenize the samples for 45 seconds. If large particles still remained, homogenization was continued until particles were no longer visible.

RNA Isolation

Immediately after homogenization, a Zymo Direct-zol RNA miniprep kit (Zymo Research, Irvine, CA) was used to isolate total RNA following procedures revised by Karishma Reddy in 2015. A Nanodrop 1000 spectrophotometer was used to measure RNA concentration (ng/µL) and absorbance ratio (260nm/280nm). The absorbance ratio was used to assess the purity of nucleic acid. The desired value of RNA purity is above 1.8; ratios less than 1.8 are considered impure and should be discarded. RNA concentration should be higher than 100 ng/µL because a lower concentration is insufficient to perform complementary DNA (cDNA) synthesis. However, some samples below 100 ng/µL were used for cDNA synthesis due to isolation limitations. Samples were stored in a -70°C freezer. Refer to Appendix A for homogenization and RNA isolation protocols and to Appendix B for sample information

$IRBP^{-/-}$ sample #2 and WT sample #1 were discarded due to their low RNA concentrations. Since $IRBP^{-/-}$ sample #4 had a small number of mice, it was combined with sample #6.1. Due to RNA yield problems, samples #5 and 6.2 and WT samples #3 and 5 were also pooled together to generate sufficient RNA concentration.

cDNA Synthesis

Complementary DNA was synthesized from RNA template (1µg or less) with an iScript cDNA Synthesis Kit and a Techne Thermal Cycler. Refer to Appencdix C for cDNA synthesis protocol, which was the procedure revised by C. DeLucia and M. Proud in summer 2013.

Primer Design

Oligonucleotide primer sequences for *c-fos* and *Bcl-x_L* were designed using gene sequences from the Nucleotide Database and (www.ncbi.nlm.nih.gov) and following protocols. Primers were obtained from Eurofins in Huntsville, AL. Another set of *c-fos* primers used by Grimm et al. was tested. The *18S* ribosomal RNA primer was previously designed by Molly Proud, and *Irbp* was designed by Molly Proud and Claire DeLucia. The *caspase-1* and *bax* primers were designed by Maggie Donaldson. Sequences and melt temperatures (T_m) are shown in Table 1.

Table 1. Primer sequences and melt temperatures (T_m)

Gene	Primer Sequence	T_m (°C)
18S rRNA Forward	ACTGACTGGCTCAGCGTGTG	59.9
18S rRNA Reverse	ACGCCAGTGTGGCCTTCTAC	59.9
Irbp Forward	GTCCTTGAGGACAACATTGG	57.85
Irbp Reverse	GGCCGGTTGTAGATCTTGTC	57.85
**c-Fos* Forward	CAACGCCGACTACGAGGCGTCAT	68.1
**c-Fos* Reverse	GTGGAGATGGCTGTCACCG	64.5
c-Fos Forward	CGACCATGATGTTCTCGGGT	62.4
c-Fos Reverse	TCGGCTGGGGAATGGTAGTA	62.4
caspase-1 Forward	CGCCCTGTTGGAAAGGAACT	62.4

caspase-1 Reverse	CCCTCAGGATCTTGTCAGCC	64.5
Bcl-x$_L$ Forward	CTGGTCGCCGGAGATAGATT	62.4
Bcl-x$_L$ Reverse	CCCGGTTGCTCTGAGACATT	62.4
bax Forward	AAACTGGTGCTCAAGGCCC	62.3
bax Reverse	CTTGGATCCAGACAAGCAGC	62.4

* Primers designed by Grimm et al. (2000)

Using the manufacturer's instructions, primers were mixed with various amounts of nuclease-free water as instructed. Then 100 µL of both forward and reverse primers for each gene were mixed with 800 µL of nuclease-free water to dilute to a concentration of 10 µM.

Quantitative Polymerase Chain Reaction (qPCR)

Following cDNA synthesis, qPCR was performed using StepOne Software version 2.0 and an Applied Biosystems 48-Well Thermal Cycler. The target genes were *c-fos, Bcl-x$_L$, bax* and *Irbp. Caspase-1* was not tested due to low amount of sample with sufficient RNA concentration. The instrument records cycle threshold (C_t), which ranges from 1 to 40 cycles, when a sufficient amount of fluorescence intensity is measured. See Appendix D for qPCR thermal cycling conditions. Each well had a total volume of 20 µL consisting of 0.5 µL cDNA, 0.5 µL of primer set, 9 µL of nuclease-free water, and 10 µL of SYBR Green Master Mix (ThermoFischer, Waltham, MA). Each primer binds to opposite ends to one transcript, and the region of the transcript between these primers is amplified. The SYBR green dye binds to double-stranded DNA and is detected with fluorescent light. Each sample and gene combination

was run in triplicate, and an average C_t was calculated. Genes that showed undetermined C_t values were re-tested. If they again showed undetermined values, then these values were neglected and only detectable values were used to calculate an average C_t. The average C_t of the 18S reference gene was subtracted from the average C_t of the target gene to calculate ΔC_t (target average C_t - reference average C_t).

Statistics

Multivariate analysis of variance (MANOVA) was used to analyze the significance of the data. This statistic test determined whether there were any differences in gene expression between WT and IRBP$^{-/-}$ mice. P-values less than 0.05 mean differences are considered significant.

Results

RNA Yield Issues

For practice samples #1 to 4, dissection and RNA isolation techniques were revised. These samples had RNA concentrations below 100 ng/µL. Since the collected RNA volume is 25 µL, RNA concentration should at least be 100 ng/µL. Therefore, these samples were discarded. $IRBP^{-/-}$ sample #2 and WT sample #1 were also discarded because their RNA concentrations were too low. Contamination was suspected in prior solutions. Therefore, a new Zymo Direct-zol RNA miniprep kit was ordered and new solutions (RNA pre-wash and RNA wash buffer) were made. The new solutions were used to isolate RNA for $IRBP^{-/-}$ sample #3 and WT sample #2. The RNA concentration for these two samples were also under 100 ng/µL. Although there was less than 1000 ng in these two samples, they were treated as if they contained 1000 ng, following all of the procedures to measure gene expression.

Retinas in $IRBP^{-/-}$ sample #6 were collected into two separate 2 mL centrifuge tubes because of a high number (13) of mice in this litter. Therefore, 6 mice (12 retinas) were collected into tube 6.1, and 7 mice (14 retinas) were collected into tube 6.2. Refer to Appendix B for sample number and number of mice used in each tube. $IRBP^{-/-}$ sample #4 and #6.1 were combined because sample #4 only contained 3 mice (6 retinas). Based on experience in the lab, a small number of retinas such as 6 typically yield a low RNA concentration. In total, combined sample #4/6.1 contained 9 mice or 18 retinas.

Given that samples regularly had low RNA concentrations, several more samples were combined, including $IRBP^{-/-}$ samples #5 and #6.2 and WT samples #4 and #5. As a result, combined $IRBP^{-/-}$ sample #5/6.2 yielded an RNA concentration of 109.2 ng/µL. Combined WT sample #4/5 yielded RNA concentration of 116.3 ng/µL.

For IRBP$^{-/-}$ sample #7, which was the last sample that were sacrificed for retina collection, its RNA concentration was 103.9 ng/µL. Even though there were only 6 mice (12 retinas) in this litter, its yield was greater than samples from litters with at least 9 mice (18 retinas. In this last sample, during RNA isolation, I modified one step in the protocol and did not disturb the pellets at all. Previously, some pellets were disturbed slightly when extracting supernatants. The RNA concentration was higher than other samples.

Gene Expression Results

Two primers for *c-Fos* were tested on IRBP$^{-/-}$ sample #1 and practice sample #5, which were all WT mice. IRBP$^{-/-}$ sample #1 was collected at night (7:30 pm). Because circadian rhythm could affect gene expression, this sample was used as a practice sample for testing primers. One primer set was designed by Grimm et al. (2000), and I designed the second primer set. Expression of *c-Fos* in IRBP$^{-/-}$ and WT mice were measured with SYBR green fluorescence by qPCR. In Table 2 the Grimm *c-fos* primer showed 5 out of 6 undetermined values. However, the primer I designed for *c-fos* (Chung) showed some detectable cycle threshold (C_t) values. These results indicate that the Chung *c-Fos* primer was more effective than the Grimm *c-fos* primer. This is probably due to a different thermal cycler program used by Grimm et al. compared to the one used at Allegheny College. Therefore, the self-designed *c-Fos* primer was used for measuring samples.

Table 2. Raw C_t values for Grimm *c-Fos* and Chung *c-Fos*

Strain	*c-Fos* (Grimm et al) (C_t)	*c-Fos* (self-designed) (C_t)
IRBP$^{-/-}$ Sample #1	Undetectable	36.84
	Undetectable	Undetectable
	Undetectable	36.96
WT Sample #5	Undetectable	35.55
	Undetectable	34.87
	37.15	36.02

Expression of *Irbp*, *Bcl-x*$_L$, and *bax* in the IRBP$^{-/-}$ and WT groups were also measured with SYBR green fluorescence by qPCR. Each target gene was measured in triplicate, and an average was calculated. Undetectable C_t values were disregarded and average was calculated between two values instead of three. Raw C_t values and melting points are provided in Appendix E. ΔC_t was calculated by subtracting the average C_t of the reference gene (*18S* ribosomal RNA*)* from the average C_t of each target gene. Average ΔC_t for genes in IRBP$^{-/-}$ and WT groups, standard deviation, and standard error of the mean (SEM) are shown in Table 3.

Table 3. ΔC_t values for target genes in IRBP$^{-/-}$ and WT mice at P25. Average ΔC_t, standard deviation, and SEM are calculated for each gene.

Strain	Sample #	*Irbp*	*c-Fos*	*Bcl-x_L*	*bax*
IRBP$^{-/-}$	3	4.49	Undetectable	Undetectable	0.127
	4/6.1	1.79	-3.23	-0.13	-2.47
	7	4.08	4.92	3.89	1.68
Average of 2 or 3 Samples		3.45	0.85 (2 s)	1.88 (2 s)	-0.22
Standard Deviation		1.19	4.08	2.01	1.71
SEM		0.67	2.35	1.16	0.99
C57BL/6J (WT)	2	-1.06	-0.94	-0.13	-2.47
	3	-0.08	2.74	1.79	-2.50
	4/5	0.27	2.52	1.70	-0.96
Average of 3 Samples		-0.29	1.46	1.12	-1.98
Standard Deviation		0.69	2.06	1.09	0.88
SEM		0.40	1.19	0.63	0.51

There is an inverse relationship between C_t value and gene expression: low C_t values (<30) mean that there is a higher gene expression than genes with higher C_t values (>34). Refer to Figure 2 for relative expression of *Irbp, c-fos, Bcl-x_L,* and *bax.* For *Irbp* in WT, the average ΔC_t appears to be higher, but not significant, than values found in the IRBP$^{-/-}$ group (ΔC_t WT -

0.29 and ΔC_t IRBP$^{-/-}$ 3.45). *c-Fos* showed barely lower expression in WT than in IRBP$^{-/-}$ (ΔC_t WT 1.458 and ΔC_t IRBP$^{-/-}$ 0.845).

Figure 2. Average delta cycle thresholds (ΔC_t) for *Irbp*, *c-Fos*, *Bcl-x$_L$*, and *bax* for P25 IRBP$^{-/-}$ (n=3) and WT (n=3) groups. Standard errors of the mean are represented by error bars. *18S* was used as a reference gene.

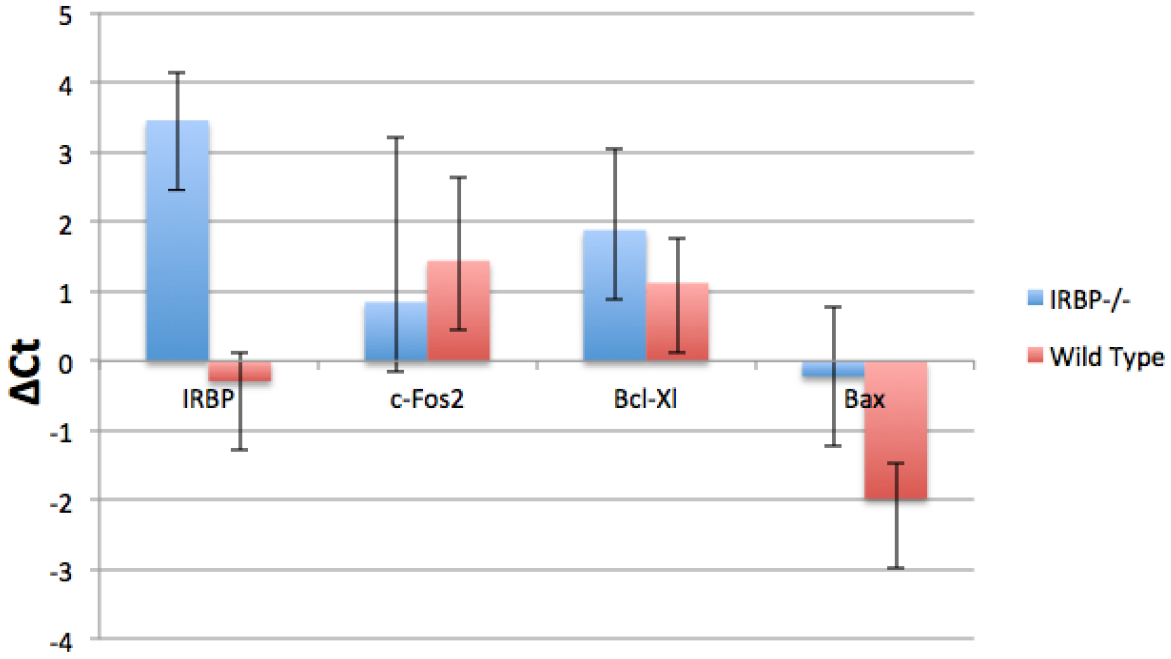

However, after multivariate analysis of variance (MANOVA) test, no significant difference was shown between IRBP$^{-/-}$ and WT groups for any genes. Table 4 shows that P-values were greater than 0.05, indicating that the hypothesis of this research was not supported.

Table 4. MANOVA: P-values for strain analysis. All 4 different statistic tests (Pillai's Trace, Wilks' Lambda, Hotelling's Trace, and Rory's Largest Root) showed p-values greater than 0.05.

Multivariate Tests

Effect		Value	F	Hypothesis df	Error df	Sig.
Intercept	Pillai's Trace	0.95	9.70[a]	4.00	2.00	.096
	Wilks' Lambda	0.049	9.70[a]	4.00	2.00	.096
	Hotelling's Trace	19.4	9.70[a]	4.00	2.00	.096
	Roy's Largest Root	19.4	9.70[a]	4.00	2.00	.096

Due to small sample size and high variability of samples in both strains, standard deviations for all genes were high. For *c-Fos* and *Bcl-x_L*, the average ΔC_t and standard deviation were calculated with two values instead of three because $IRBP^{-/-}$ sample #3 had undetectable values.

Negative values for average ΔC_t were calculated for *Irbp* in WT (-0.29) and *bax* in both $IRBP^{-/-}$ and WT groups (-0.222 and -1.98). The negative sign means that these genes were expressed at a cycle earlier when the reference gene, *18S* ribosomal RNA appeared. *Bax* consistently showed more expression than the reference gene in all three samples in WT groups. Due to insigficant difference, both groups showed similar level of *bax* expression.

Discussion

The goal of this research was to investigate whether genes that play a role in inducing photoreceptor apoptosis activated from exposure to high light intensity have higher expression in IRBP$^{-/-}$ mice, without exposing the animals to light, compared to WT mice. Through high intensity light treatment, which damaged photoreceptors, Grimm et al. found that *c-Fos* mRNA levels were increased (2000). Therefore, it was concluded that c-Fos plays a strong role in activating AP-1 transcription factor to induce murine photoreceptor apoptosis. Similarly, this research tested for gene expression of pro-apoptotic genes c-Fos and bax and anti-apoptotic gene *Bcl-x$_L$*. This research hypothesized that there would be higher expression of *c-Fos, caspase-1*, and *bax* and lower expression of *Bcl-x$_L$* in 25-day-old IRBP$^{-/-}$ mice compared to age-matched WT mice. As mentioned previously, due to insufficient RNA concentration (<100 ng/µL), *caspase-1* was not tested.

Gene expression was measured using qPCR. *Irbp* tended to be higher expression in WT than in IRBP$^{-/-}$ mice. This was expected because IRBP$^{-/-}$ mice lack functional IRBP (ΔC_t WT - 0.29 +/- 0.689 and ΔC_t IRBP$^{-/-}$ 3.45 +/- 1.19). Although, not reaching statistical significance, this result indicates that IRBP$^{-/-}$ mice are still deficient in *Irbp* gene and appear to have been breeding completely isolated from WT mice in the Allegheny College colony. A previous comp student, Abbey Turner, observed a similar trend. Turner's ΔC_t value of *Irbp* in IRBP$^{-/-}$ group was 15.86 and in WT group was 12.67 (2016). Her results also indicate that IRBP$^{-/-}$ mice lack functional IRBP compared to WT mice.

Gene expression of *c-Fos* was somewhat higher in the IRBP$^{-/-}$ group than the WT group. Although the results did not reach statistical difference, this trend is consistent with my hypothesis. Grimm et al (2000) showed that there was a high expression of *c-Fos* in WT mice

after exposure to high light intensity, which activates AP-1. They concluded that photoreceptor degeneration was occuring due to activation of AP-1 (Grimm et al., 2000). IRBP$^{-/-}$ mice undergo photoreceptor degeneration around postnatal day 23 (Wisard et al., 2011). It is unknown whether the apoptosis of IRBP$^{-/-}$ mice uses the same pathway as AP-1. However, the results in this experiment are suggestive that *c-Fos*, which is one of the key players in AP-1 transcription factor, is experienced in retinas of IRBP$^{-/-}$ mice. In conclusion, because the results did not reach statistical difference, no difference of the mean between IRBP$^{-/-}$ and WT group is found for *c-Fos.*

Given that IRBP$^{-/-}$ mice undergo apoptosis, I hypothesized that *Bcl-x$_L$* would have lower expression and *bax* would have higher expression in IRBP$^{-/-}$ group compared to WT. Figure 2 shows a similar level of expression of *Bcl-x$_L$* in IRBP$^{-/-}$ than WT. *Bax* also showed similar level of expression in IRBP$^{-/-}$ mice than in WT, which is inconsistent with my hypothesis. A possible explanation for why the pro-apoptotic *bax* had similar level of expression in IRBP$^{-/-}$ mice relates to peak apoptosis occuring between p23 and p30 in IRBP$^{-/-}$ mice (Wisard et al., 2011). Among three ages (p23, p25, and p27), p25 showed the most TUNEL-positive cells in IRBP$^{-/-}$ mice. However, this does not agree with my results with *bax* expression. It could be that my IRBP$^{-/-}$ mice reached their peak of photoreceptor apoptosis at a day or two earlier or later than p25. Then apoptosis decreased at p25, resulting in reduced expression of *bax* (pro-apoptotic gene). Also, there could be reduced expression of *c-Fos*, if the peak of apoptosis occurred before or after p25. Another possibility is that *c-Fos* has no role in the IRBP$^{-/-}$ mice.

Negative ΔC_t values for *bax* in both IRBP$^{-/-}$ and WT mice indicates that *bax* has higher expression than the reference gene. For WT, all three samples consistently showed higher expression of *bax* than *18S.* If the low RNA concentration of samples IRBP$^{-/-}$ sample # 2 and WT

sample # 2/3 resulted in the low expression of *18S*, then the other genes should also have low expression. *Bax* ΔC_t values were compared to previous comp students *bax* values. Linnea Homa had ΔC_t of 4.29 for *bax* in IRBP$^{-/-}$ group and 3.45 in WT group (2013). Her positive ΔC_t values for *bax* in both groups indicate that her *18S* gene had higher expression than *bax,* which disagrees with my data. My ΔC_t values for both IRBP$^{-/-}$ and WT groups were negative. However, comparing my data to Homa's data still does not explain why my *bax* had higher expression than the reference gene.

Conclusion

Although a trend may have appeared in my results as I predicted, none of the comparisons reached statistical significance, meaning that the groups did not have different gene expression. Expression of *c-Fos* in IRBP$^{-/-}$ compared to WT group shows inconsistency with my prediction that *c-Fos* may play a role in photoreceptor degeneration in IRBP$^{-/-}$ mice. Given that my p-values are greater than 0.05, this research concludes that *c-Fos* is not observed in IRBP$^{-/-}$ mice. Furthermore, pro-apoptotic gene *bax* in IRBP$^{-/-}$ mice shows similar level of expression compared to WT mice. Further experimentation can be done by testing for *c-Jun,* which is another key player in light-induced apoptosis via activation of AP-1. Also, *caspase-1* should be tested and compared to *c-fos* expression. Although it is still not well understood how *caspase-1* is involved in AP-1 transcription, high expression of *caspase-1* was observed in light-induced photoreceptor degeneration (Grimm et al., 2000). Therefore testing for *caspase-1* in IRBP$^{-/-}$ mice would help to determine whether IRBP$^{-/-}$ mice and high light intensity exposed mice share a similarity in their mechanism of photoreceptor apoptosis.

Literature Cited

Ameyar, M., Wisniewska, M., & Weitzman, J. B. (2003). A role for AP-1 in apoptosis: The case for and against. *Biochimie, 85*(8), 747-752.

Doonan, F., Maryanne D., & Thomas G. C. (2003). "Caspase-Independent Photoreceptor Apoptosis in Mouse Models of Retinal Degeneration." *Journal of Neuroscience* 23.13

Elmore, S. (2007). Apoptosis: A review of programmed cell death. *Toxicologic Pathology, 35*(4), 495-516.

Gavrilescu, L. C., & Denkers, E. Y. (2003). Apoptosis and the balance of homeostatic and pathologic responses to protozoan infection. *Infection and Immunity, 71*(11), 6109-6115.

Grimm, C., Wenzel, A., Hafezi, F., & Remé, C. E. (2000). Gene expression in the mouse retina: The effect of damaging light. *Molecular Vision, 6*, 252-260.

Hafezi, F., Marti, A., Grimm, C., Wenzel, A., & Remé, C. E. (1999). Differential DNA binding activities of the transcription factors AP-1 and oct-1 during light-induced apoptosis of photoreceptors. *Vision Research, 39*(15), 2511-2518.

Homa, L. (2013). Expression of Genes Involved in the Regulation of the Intrinsic Apoptotic. Pathway in IRBP-/- Mus musculus. Allegheny College Senior Comprehensive Project.

Keating, A. M., Garlipp, M., & Gonzalez-Fernandez, F. (2008). Interphotoreceptor retinoid-binding protein (IRBP) binds cone outer segments differentially in light and dark adapted xenopus retina. *Invest. Ophthalmol. Vis. Sci., 49*(13), 3531-3531.

Kroemer, G., Galluzzi, L., Vandenabeele, P., Abrams, J., Alnemri, E., Baehrecke, E., … Melino, G. (2009). Classification of cell death: recommendations of the Nomenclature Committee on Cell Death 2009. *Cell Death and Differentiation*, *16*(1), 3–11.

Liou GI, Wang M, & Matragoon S. (1994). Timing of interphotoreceptor retinoid binding protein (IRBP) gene expression and hypomethylation in developing mouse retina. *Dev Biol.*

Liu, X., Kim, C. N., Yang, J., Jemmerson, R., & Wang, X. (1996). Induction of apoptotic program in cell-free extracts: Requirement for dATP and cytochrome c. *Cell, 86*(1), 147-157.

Livingston, D. J.(1997). "In Vitro and in Vivo Studies of ICE Inhibitors." Journal of cellular biochemistry 64.1

National Eye Institute. (2014). Facts About Retinitis Pigmentosa. Web. 14 Dec. 2016.

Parker, R. O., Fan, J., Nickerson, J. M., Liou, G. I., & Crouch, R. K. (2009). Normal cone function requires the interphotoreceptor retinoid binding protein. *Journal of Neuroscience, 29*(14), 4616.

Pepperberg, D.R., Okajima, T.L., Wiggert, B., Ripps, H., Crouch, R.K., & Chader, G.J. (1993). Interphotoreceptor retinoid-binding protein (IRBP) molecular biology and physiological role in the visual cycle of rhodopsin. *Molec. Neurobio*.: 7(1); 61-84.

Perche, O., Michel D., & Isabelle, Ranchon-C. (2007). "Caspase-Dependent Apoptosis in Light-I nduced Retinal Degeneration." *Invest. Ophthalmology & Visual Science* 48.6: 2753-9.

Tsujimoto, Y. (1998). Role of bcl-2 family proteins in apoptosis: Apoptosomes or mitochondria? *Genes to Cells: Devoted to Molecular & Cellular Mechanisms*, *3*(11), 697-707.

Turner, A. (2016). Anti-Apoptotic Gene Expression in the Mouse Retina During Early Ocular Development. Allegheny College Senior Comprehensive Project.

Wisard, J., Faulkner, A., Chrenek, M. A., Waxweiler, T., Waxweiler, W., Donmoyer, C., . . . Nickerson, J. M. (2011). Exaggerated eye growth in IRBP-deficient mice in early development. *Invest. Ophthalmol. Vis. Sci.*, *52*(8), 5804-5811.

Zhivotovsky, B. (2003). Caspases: The enzymes of death. *Essays in Biochemistry*, *39*, 25

Appendix A

Homogenization and RNA Isolation Protocol

Homogenization

1. Add 500 µL Trizol to sample in 2.0mL centrifuge tube
2. Homogenize until tissue fragments are no longer visible with a Kontes pellet pestle motor.

RNA Isolation – Zymo Direct-zol RNA Miniprep Kit Protocol

1. Centrifuge homogenized sample at 13,000 rpm for 1 minute
2. Do not disturb the pellet, transfer supernatant into a new sterile 2mL centrifuge tube.
3. Discard pellet
4. Add an equal volume of 95% ethanol and vortex until homogeneous
5. Transfer mixture without disturbing pellet into a Zymo spin column in a collection tube
6. Centrifuge at 13,000 rpm for 1 minute
8. Discard flow through in sink and add 400 µL of Direct-zol RNA pre Wash to the column. Centrifuge at 13,000 rpm for 1 minute
9. Dispose of follow through and repeat step 7
10. Add 700 µL of RNA wash buffer to the column. Centrifuge at 13,000 rpm for 1 minute.
11. Discard collection tube and place column in a new 2mL centrifuge tube
12. Add 25 µL of nuclease-free water to the column to elute RNA
13. Discard column and measure RNA concentration and purity with Nanodrop spectrophotometer.

Appendix B

Sample #	IRBP$^{-/-}$	C57	Practice Sample
1	*9 mice RNA: 112.9 ng/µL Purity: 1.82	7 Mice RNA: 25.0 ng/µL Purity 1.6	8 Mice RNA: 24.6 ng/µL Purity: 1.86
2	8 Mice RNA: 12.1 ng/µL Purity: 1.72	8 Mice RNA: 58.2 ng/µL Purity: 1.8	4 Mice RNA: 44.6 ng/µL Purity 1.86
3	6 Mice RNA: 19.3 ng/µL Purity: 1.93	8 Mice RNA: 44.5 ng/µL Purity: 1.94	6 Mice RNA: 54.2 ng/µL Purity: 1.82
4	**3 Mice See #6.1	****7 Mice See #5	5 Mice RNA: 26.2 ng/µL Purity: 1.82
5	***9 Mice	****10 Mice with #4 RNA: 116.3 ng/µL Purity: 1.90	7 Mice RNA: 98.5 ng/µL Purity: 1.78
6.1	**6 Mice with #4 RNA: 79.3 ng/µL Purity: 1.82		
6.2	***7 Mice with #5 RNA: 109.2 ng/µL 1.79		
7	6 Mice RNA: 103.9 ng/µL Purity: 1.8		

* Sample was collected at 7:30 pm

** Samples were pooled together

*** Samples were pooled together

**** Samples were pooled together

Appendix C

1. Calculate the volume of RNA template needed using the following equation

   If RNA concentration below 200 ng/µL

   200 ng/µL = 1000 ng/ x µL
   X = 5 µL

2. Obtain and label one microcentrifuge tube, using the following protocol:

Reagent	Volume per Reaction
5x iScript Reaction Mix	4 µL
Nuclease free water	16 - x µL
RNA template	X µL
Total Volume	20 µL

3. Vortex tube and incubate in Techne thermal cycler. Select MOLLYCLAIRE program.

MOLLYCLAIRE program conditions:

25°C: 5 min

42°C: 30 min

85°C: 5 min

4°C: Final hold

Appendix D

Conditions for quantitative Real-Time Polymerase Chain Reaction

Holding stage: 95°C: 10 min

Annealing and elongation stage: (40 cycles)

95°C: 15 min

60°C: 1 min

Melt curve analysis:

95°C: 15 min

60°C: 1 min

95°C: 15 min

Appendix E

qPCR Raw Cycle Threshold (C_t) Values and melt temperatures (T_m)

Sample	Target	C_t	T_m
IRBP$^{-/-}$ #3	*18S*	30.9	80.19
IRBP$^{-/-}$ #3	*18S*	31.7	79.0
IRBP$^{-/-}$ #3	*18S*	30.7	80.2
IRBP$^{-/-}$ #3	*Irbp*	35.3	70.9
IRBP$^{-/-}$ #3	*Irbp*	37.2	70.9
IRBP$^{-/-}$ #3	*Irbp*	34.4	70.9
IRBP$^{-/-}$ #3	*c-Fos*	Undetectable	86.0
IRBP$^{-/-}$ #3	*c-Fos*	Undetectable	85.4
IRBP$^{-/-}$ #3	*c-Fos*	Undetectable	61.3
IRBP$^{-/-}$ #3	*Bcl-x$_L$*	Undetectable	61.6
IRBP$^{-/-}$ #3	*Bcl-x$_L$*	Undetectable	61.6
IRBP$^{-/-}$ #3	*Bcl-x$_L$*	Undetectable	61.6
IRBP$^{-/-}$ #3	*bax*	31.32	71.7
IRBP$^{-/-}$ #3	*bax*	31.28	71.7
IRBP$^{-/-}$ #3	*bax*	31.11	71.8
IRBP$^{-/-}$ #4/6.1	*18S*	34.6	78.9
IRBP$^{-/-}$ #4/6.1	*18S*	36.1	78.9
IRBP$^{-/-}$ #4/6.1	*18S*	36.7	78.9
IRBP$^{-/-}$ #4/6.1	*Irbp*	39.1	71.0
IRBP$^{-/-}$ #4/6.1	*Irbp*	37.0	71.0
IRBP$^{-/-}$ #4/6.1	*Irbp*	36.7	71.1
IRBP$^{-/-}$ #4/6.1	*c-Fos*	Undetectable	85.6

IRBP$^{-/-}$ #4/6.1	*c-Fos*	32.6	83.6
IRBP$^{-/-}$ #4/6.1	*c-Fos*	Undetectable	85.6
IRBP$^{-/-}$ #4/6.1	*Bcl-x$_L$*	Undetectable	86.2
IRBP$^{-/-}$ #4/6.1	*Bcl-x$_L$*	Undetectable	86.2
IRBP$^{-/-}$ #4/6.1	*Bcl-x$_L$*	Undetectable	86.2
IRBP$^{-/-}$ #4/6.1	*bax*	32.5	71.7
IRBP$^{-/-}$ #4/6.1	*bax*	32.4	71.6
IRBP$^{-/-}$ #4/6.1	*bax*	32.5	71.7
IRBP$^{-/-}$ #7	*18S*	32.3	80.5
IRBP$^{-/-}$ #7	*18S*	31.9	80.3
IRBP$^{-/-}$ #7	*18S*	30.9	80.3
IRBP$^{-/-}$ #7	*Irbp*	37.0	61.7
IRBP$^{-/-}$ #7	*Irbp*	35.5	70.7
IRBP$^{-/-}$ #7	*Irbp*	34.9	70.8
IRBP$^{-/-}$ #7	*c-Fos*	36.1	83.6
IRBP$^{-/-}$ #7	*c-Fos*	36.9	83.6
IRBP$^{-/-}$ #7	*c-Fos*	36.9	83.7
IRBP$^{-/-}$ #7	*Bcl-x$_L$*	35.5	62.0
IRBP$^{-/-}$ #7	*Bcl-x$_L$*	35.3	62.0
IRBP$^{-/-}$ #7	*Bcl-x$_L$*	36	62.0
IRBP$^{-/-}$ #7	*bax*	33.9	71.7
IRBP$^{-/-}$ #7	*bax*	33.4	71.8
IRBP$^{-/-}$ #7	*bax*	32.9	71.8
WT #2	*18S*	35.9	62.2
WT #2	*18S*	35.9	62.3
WT #2	*18S*	37.0	85.6

WT #2	*Irbp*	35.3	70.7
WT #2	*Irbp*	34.6	70.8
WT #2	*Irbp*	35.7	70.8
WT #2	*c-Fos*	37.0	62.6
WT #2	*c-Fos*	Undetectable	85.7
WT #2	*c-Fos*	33.6	61.6
WT #2	*Bcl-x_L*	35.1	76.5
WT #2	*Bcl-x_L*	36.2	62.8
WT #2	*Bcl-x_L*	37.1	62.8
WT #2	*bax*	33.7	71.4
WT #2	*bax*	33.7	71.4
WT #2	*bax*	34.0	71.3
WT #3	*18S*	33.6	78.7
WT #3	*18S*	32.6	80.4
WT #3	*18S*	37.1	78.7
WT #3	*Irbp*	34.0	70.8
WT #3	*Irbp*	37.2	71.3
WT #3	*Irbp*	31.9	71.0
WT #3	*c-Fos*	Undetectable	61.4
WT #3	*c-Fos*	37.2	72
WT #3	*c-Fos*	Undetectable	61.4
WT #3	*Bcl-x_L*	37.0	73.9
WT #3	*Bcl-x_L*	35.4	73.3

WT #3	*Bcl-x_L*	Undetectable	85.6
WT #3	*bax*	31.6	71.7
WT #3	*bax*	31.9	71.7
WT #3	*bax*	32.3	71.7
WT #4/5	*18S*	35.8	80.0
WT #4/5	*18S*	37.1	78.4
WT #4/5	*18S*	30.2	79.4
WT #4/5	*Irbp*	37.6	70.4
WT #4/5	*Irbp*	33.1	70.8
WT #4/5	*Irbp*	33.2	70.8
WT #4/5	*c-Fos*	38.3	84.2
WT #4/5	*c-Fos*	36.0	62.5
WT #4/5	*c-Fos*	36.3	62.3
WT #4/5	*Bcl-x_L*	37.0	61.7
WT #4/5	*Bcl-x_L*	35.8	61.7
WT #4/5	*Bcl-x_L*	35.4	61.7
WT #4/5	*bax*	33.9	71.7
WT #4/5	*bax*	33.4	71.5